

Supporting Information

Multifunctional SA-PProDOT Binder for Lithium Ion Batteries

*Min Ling,^{a,d} Jingxia Qiu,^a Sheng Li,^a Cheng Yan,^b Milton J. Kiefel,^c Gao Liu,^{*d} and Shanqing
Zhang^{*a}*

^a Centre for Clean Environment and Energy, Environmental Futures Research Institute and
Griffith School of Environment, Griffith University, Gold Coast Campus, Queensland 4222,
Australia

^b School of Chemistry, Physics and Mechanical Engineering, Queensland University of
Technology, Brisbane, Queensland 4001, Australia

^c Institute for Glycomics, , Griffith University, Gold Coast Campus, Queensland 4222, Australia

^d Environmental Energy Technologies Division, Lawrence Berkeley National Laboratory,
Berkeley, California 94720, United States

Materials

Sodium alginate (SA) was purchased from MP Biomedicals (Catalog No. 154724). 3,4-propylenedioxythiophene-2,5-dicarboxylic acid (ProDOT) was purchased from Sigma-Aldrich (Product No. 660477) and used without further purification. Electrolytes, that is, 1 M LiPF₆ in

EC and dimethyl carbonate (DMC) (1/1 w/w), were purchased from Ferro Corp.

SA-PProDOT synthesis

The microemulsion system was prepared by addition of the 50 mmol/L of dodecyl benzenesulfonic acid (DBSA) into 10 ml cyclohexane and subsequent a pH 7.0 buffer was added at water to surfactant weight ratio ω_o ($m_{H_2O}/m_{\text{surfactant}}$) of 5 resulted in a creamy solution. The molar ratio of ProDOT in the polymer is 50% while the weight ratio of ProDOT in the polymer is 55.4%. The concentration of $FeCl_3$ for polymerization is 0.5 wt%. Under continuous stirring, 197 mg SA and 244.23 mg ProDOT were added into the microemulsion system and subsequently refluxed under vigorous stirring for 24 h at room temperature. The resultant product was obtained after evaporation of the solvents in rotary evaporator.

Electrochemical evaluation

The as-prepared SA-PProDOT polymer was dispersed in NMP to 40 mg/ml and mixed with $LiFePO_4$ (LFP) at designed weight ratios, resulting in SA-PProDOT slurry. SA and PVDF are used to prepare control samples with the identical ratios, namely SA and PVDF samples.

It is well-recognized that the side reaction between H_2O and the electrolyte causes dramatic deterioration of electrolyte and leads to the loss of cell performance. In order to avoid this side reaction, the water content was strictly controlled by drying treatment of the electrode at $110^\circ C$ in a vacuum oven and assembly of the batteries in an Ar-filled glove box (<0.1 ppm water). The loading on each aluminum foil is ca. 3 mg/cm^2 .

The electrochemical behaviour of the electrodes was tested in coin cells in terms of galvanostatic discharge-charge cycling tests at ambient temperature using a LANDdtes

Instrument Testing System. All current density and specific capacity calculations are based on the active mass of LFP. The CR2032 coin cells were assembled using a lithium foil as a counter electrode and 1.0 M LiPF₆ in a 1:1 mixture of ethylene carbonate (EC) and dimethyl carbonate (DMC) as the liquid electrolyte (Ferro Corp., USA battery grade). All the above reported procedures were performed in the inert atmosphere of an Ar-filled dry glove box (MBraun Labstar, O₂ and H₂O content ≤ 0.1 ppm). The coin cells were storing in thermal chamber at 55 °C for a period to investigate the self-discharge rate. Before placing in thermal chamber, the cells were subjected to the formation process by applying 5 full cycles at 25 °C with 1 C rate.

Materials Characterisation

Composite electrode surface images were collected with JEOL 7001F field emission scanning electron microscopy. The in-lens secondary electron detector was used for the studies. Most of which were performed using an accelerating voltage of 5 kV and a working distance of 2-5 mm. Kratos Axis ULTRA X-ray Photoelectron Spectrometer (XPS) incorporating a 165 mm hemispherical electron energy analyser was used to obtain XPS spectra of the samples. The incident radiation was Monochromatic Al K α X-rays (1486.6 eV) at 225 W (15 kV, 15 ma). Survey (wide) scans were conducted with at 160 eV while multiplex (narrow) high resolution scans at 20 eV. Survey scans were carried out in a 1200-0 eV binding energy range with 1.0 eV steps and a dwell time of 100ms. Narrow high-resolution scans were run with 0.05 eV steps and 250 ms dwell time. Base pressure in the analysis chamber was 1.0x10⁻⁹ torr and during sample analysis 1.0x10⁻⁸ torr. Atomic concentrations were calculated using the CasaXPS version 2.3.14 software and a Shirley baseline with Kratos library Relative Sensitivity Factors (RSFs). Peak fitting of the high-resolution data was also carried out using the CasaXPS software. All binding

energies were referenced to the C1s peak 285.0 eV.

Adhesion measurements of the electrodes were performed on a Chatillon® TCD225 series force measurement system. The Cu side of graphite electrode (1 cm × 1 cm) was fixed vertically to the bottom sample holder. The adhesive side of a Scotch Magic® tape was firmly applied onto the electrode laminate side. The tape was peeled off using the top sample holder at the direction of 180° angle to the adhered tape and parallel to one side of the electrodes, and at 10 inch min⁻¹ moving rate to the bottom sample holder. The first data point of each test, between 0 and 0.05 cm, corresponds to the beginning of the tape tension, with the forced offset to zero. When the tension is fully applied, the measured force value reaches a plateau, representing the adhesion force of the electrode laminates.

The compatibility of the binder with the electrolyte solvent was examined by a swelling test. Binder sheets were prepared by solution-cast samples and the solvents were removed in a vacuum oven at 80 °C overnight. Binder sheets were then placed in EC/DMC (1/1 w/w) electrolyte at room temperature. The swelling ratio was defined as the weight ratio of the amount of absorbed solvent to the dry weight of the tested binder sheet.

Fourier Transform Infrared (FTIR) spectroscopy measurements were performed using a Thermo- Nicolet (Thermo Electron Corporation, USA) Magna 550 FTIR spectrometer equipped with a Thermo-Nicolet Nic-Plan FTIR microscope. For each spectrum 32 scans were collected at a resolution of 4 cm⁻¹ from 4000 cm⁻¹ to 500 cm⁻¹. All the FTIR data were analysed using OMNIC E.S.P version 6.1a software (Thermo Scientific, USA).

In nanoscratch tests, a conical indenter (with radius approximately 1 μm, 90° cone angle) was used to scratch over the sample surface for obtaining friction coefficient information of each sample. During the scratch process, the normal load was kept constant as 500 μN and the lateral

displacement was set as 12 μm .

The nanoindentation tests were undertaken using Hysitron TI 950 nanoindentation system with Berkovich indenter (three-sided pyramidal tip with radius approximately 150nm, 142.3 ° total included angles).

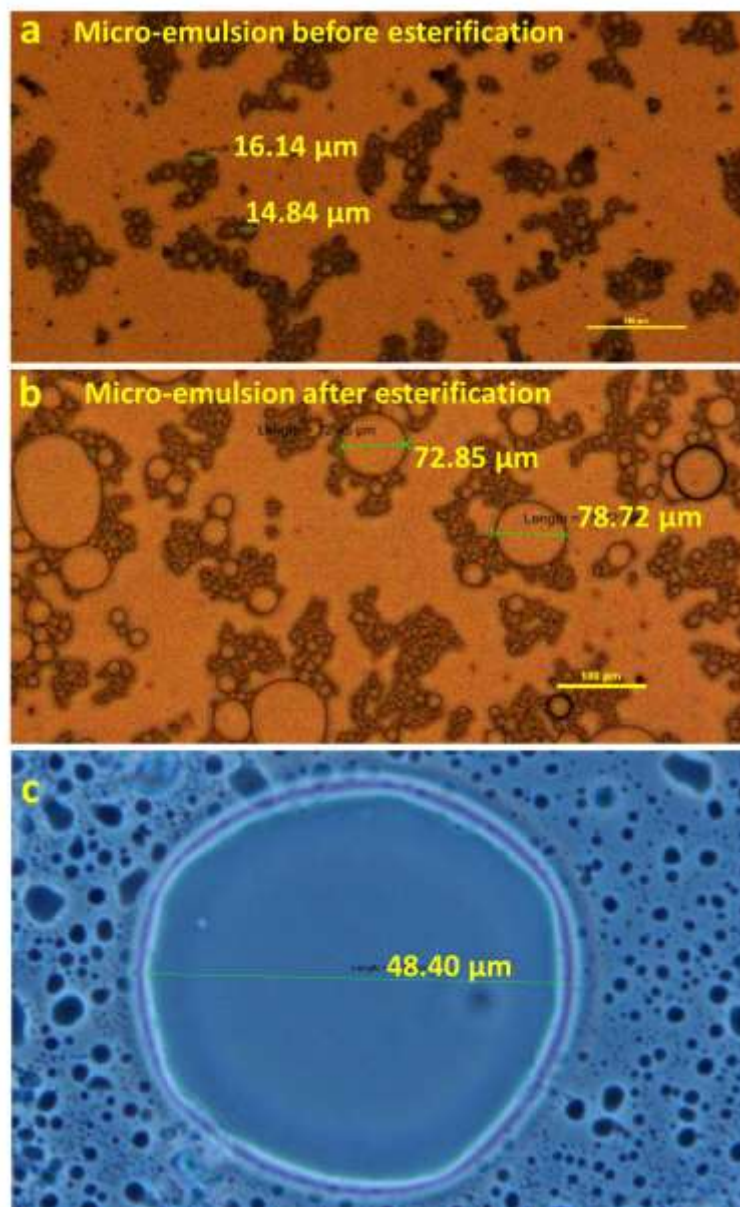


Figure S1. (a) Optical microscopy image of cyclohexane/DBSA/water microemulsion system. (b,c) The average water droplets diameter increases after the esterification between SA and ProDOT.

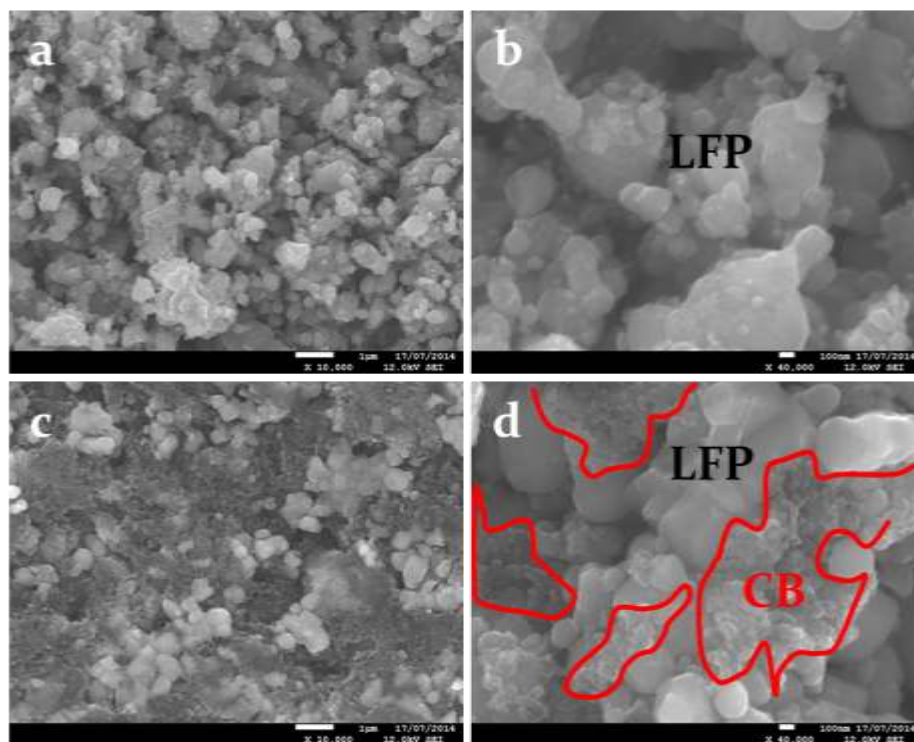


Figure S2. SEM images of the LiFePO_4 (LFP) electrodes based on (a, b) SA-PProDOT (LFP:binder=8:2) and (c, d) PVDF binder (LFP:PVDF:CB=8:1:1).

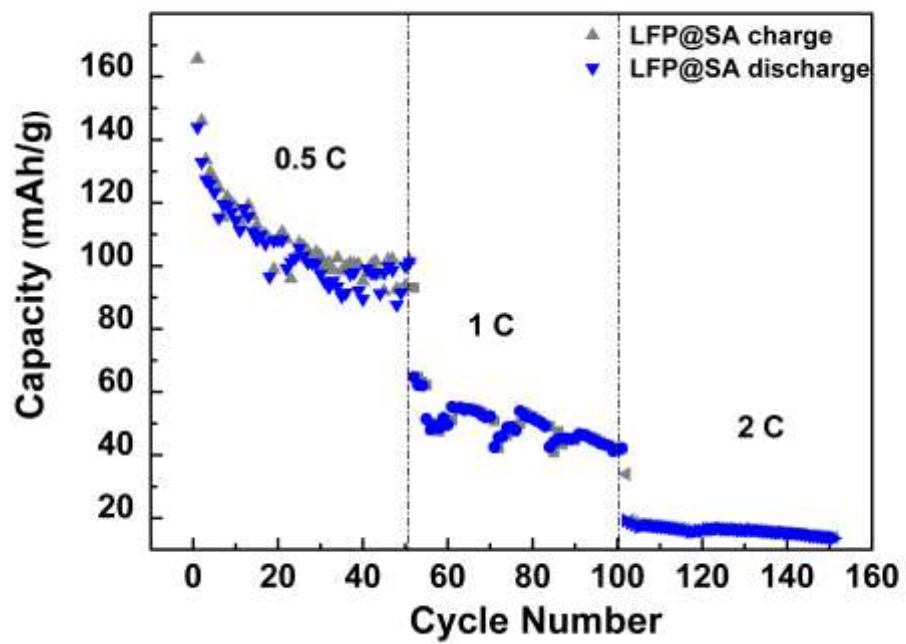


Figure S3. Discharge-charge curve for sodium alginate binder based LFP electrode (LFP:SA:CB=8:1:1).

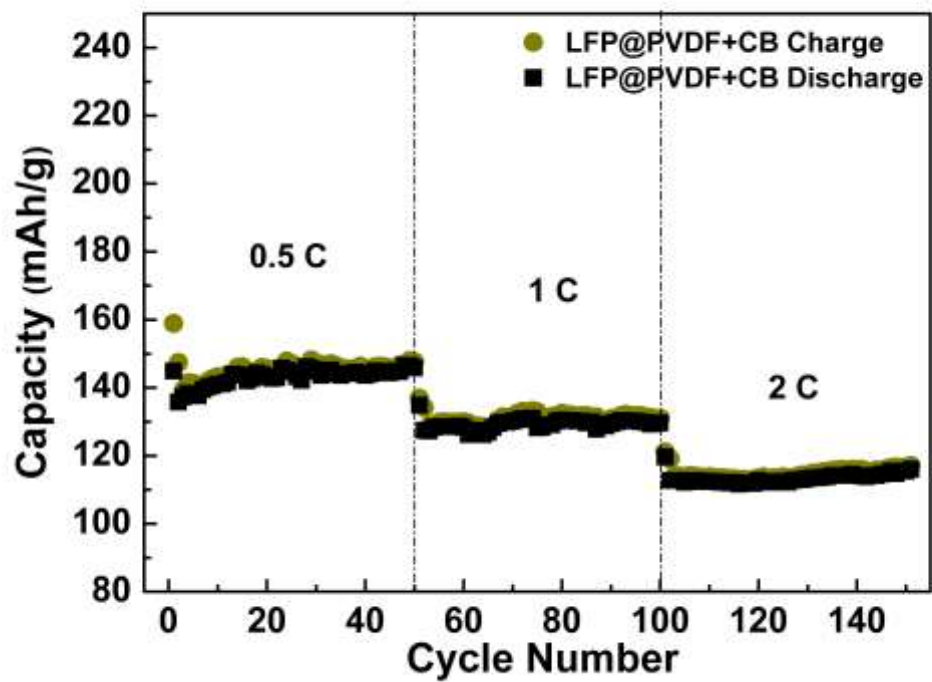


Figure S4. Electrochemical performance of a LiFePO_4 electrode based on PVdF binder at vary C rate between a cycling voltage of 2.0 and 4.2 V (LFP:PVDF:CB=8:1:1).

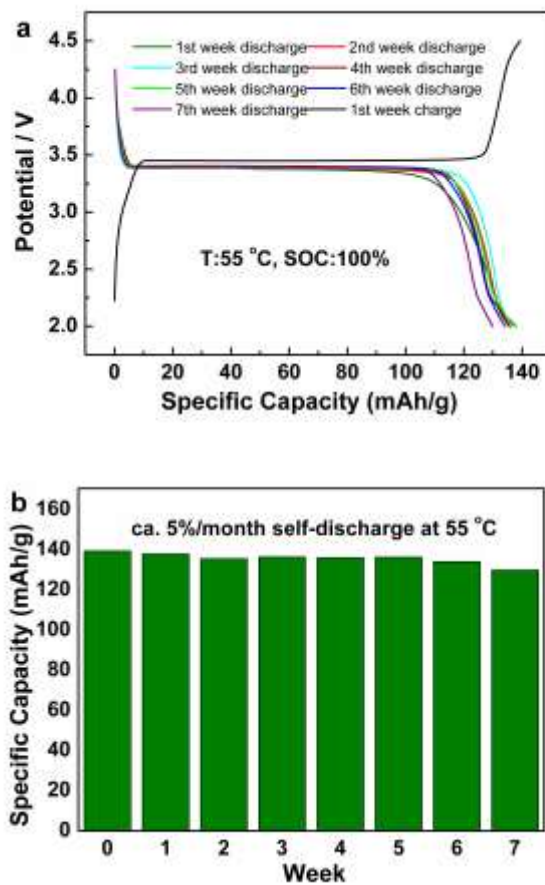


Figure S5 (a) Discharge-charge curves profile for self-discharge test on LFP@SA-PProDOT cells at 1 C rate. (b) Capacity evolution after storage at 55 °C for 7 weeks.

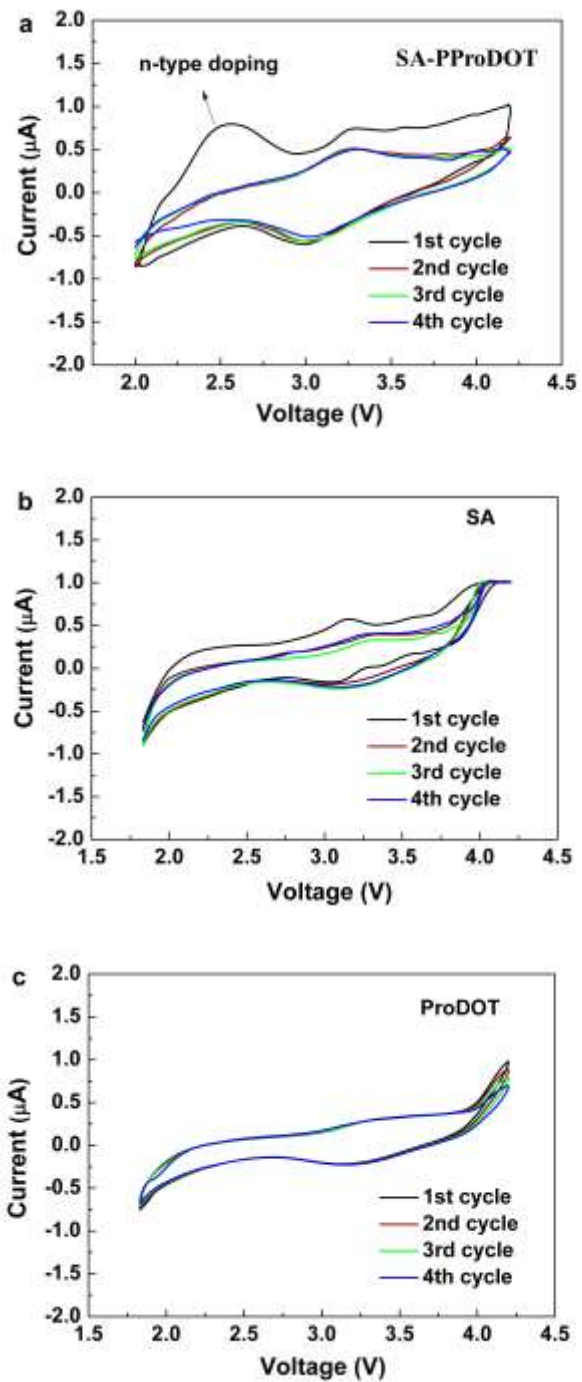


Figure S6. Cyclic Voltammograms of the SA-PProDOT, SA and PProDOT thin film in lithium ion electrolyte at the rate of 0.2 mV/s, respectively.

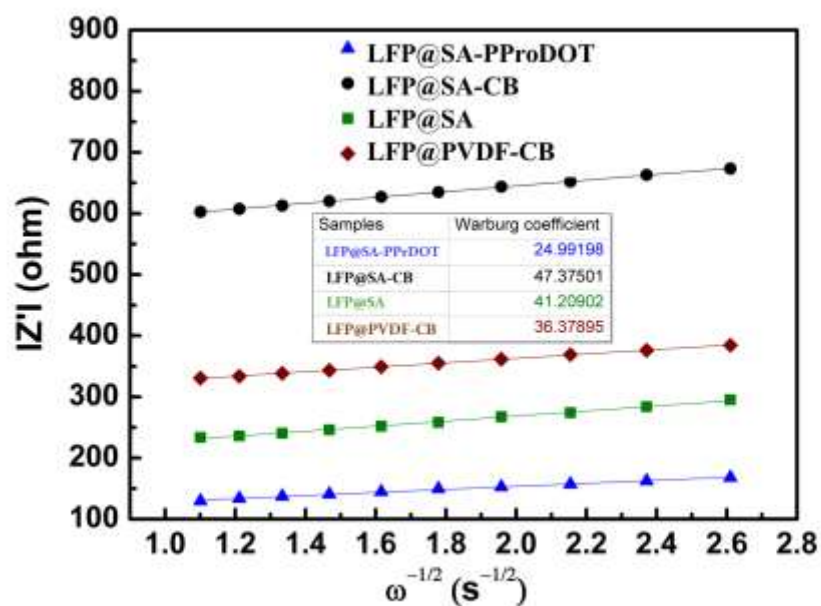


Figure S7. Warburg coefficient σ_w calculated by the plot of Z' vs. the reciprocal square roots of the lower angular frequencies (ω).

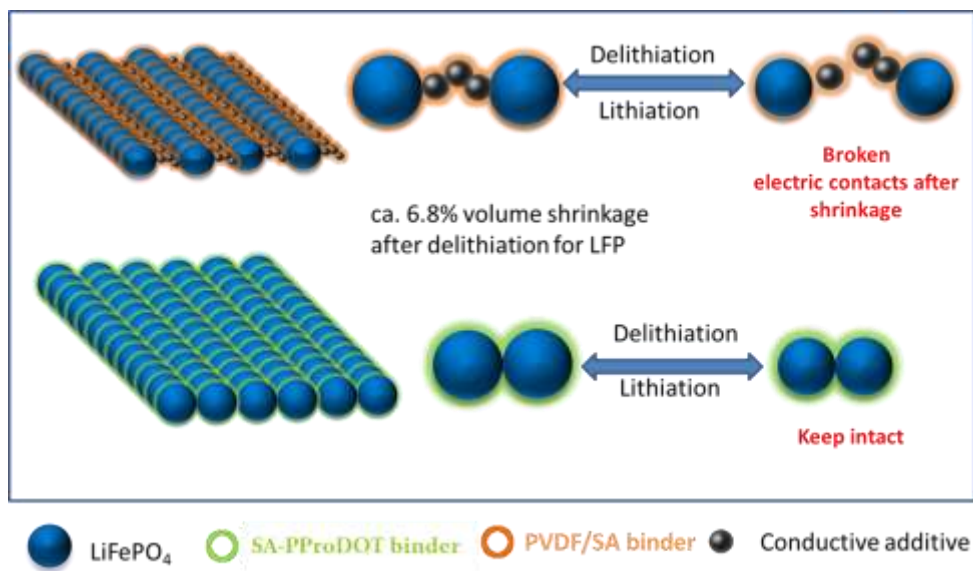


Figure S8. The electrical conduction mechanisms at the electrodes with the conventional PVDF and SA-PProDOT polymer binder in the lithiation/delithiation processes.

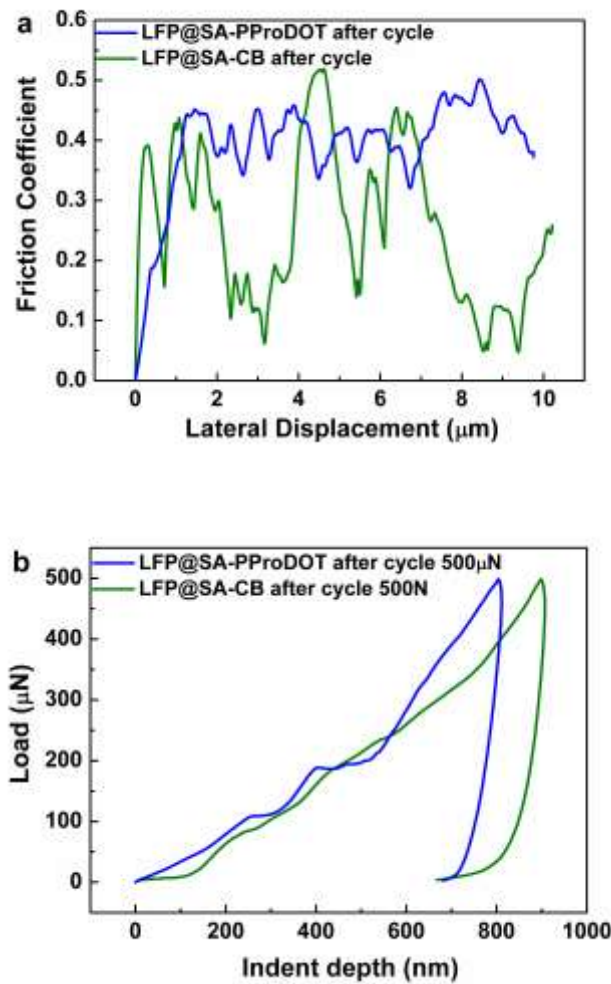


Figure S9 (a) Nanoscratch tests for cycled LFP@SA-PProDOT and LFP@SA-CB electrodes (after electrolyte uptake). (b) Nanoindentation tests for cycled LFP@SA-PProDOT and LFP@SA-CB electrodes (after electrolyte uptake).

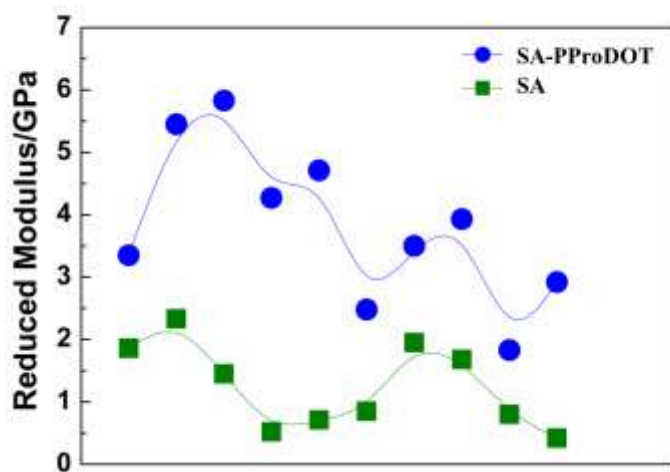


Figure S10. Average reduced modulus variations of the SA and SA-PProDOT polymers obtained by the nanoindentation test under 2000 μN for ten individual indents.